



ELSEVIER

Engineering Geology 52 (1999) 231–250

ENGINEERING  
GEOLOGY

## Mathematical modelling of groundwater flow at Sellafield, UK

Chris McKeown<sup>1, \*</sup>, R. Stuart Haszeldine<sup>2</sup>, Gary D. Couples<sup>1</sup>

*Geology and Applied Geology, University of Glasgow, Glasgow, G12 8QQ, UK*

---

### Abstract

Sellafield in West Cumbria was a potential site for the location of the UK's first underground repository for radioactive, intermediate level waste (ILW). The repository was to lie around 650 m beneath the ground surface within rocks of the Borrowdale volcanic group (BVG), a thick suite of SW dipping, fractured, folded and metamorphosed Ordovician meta-andesites and ignimbrites. These are overlain by an onlapping sequence of Carboniferous and Permo-Triassic sediments. In situ borehole measurements showed that upward trending fluid pressure gradients exist in the area of the potential repository site, and that there are three distinct fluid types in the subsurface; fresh, saline and brine (at depth, to the west of the site). Simulations of fluid flow in the Sellafield region were undertaken with a 2D, steady-state, coupled fluid and heat flow simulation code (OILGEN). In both simplified and geologically complex models, topographically driven flow dominated the regional hydrogeology. Fluids trended persistently upwards through the potential repository site. The dense brine to the west of the site promoted upward deflection of topographically driven groundwaters. The inclusion in hydrogeological models of faults and variably saline sub-surface fluids was essential to the accurate reproduction of regional hydraulic head variations. Sensitivity analyses of geological variables showed that the rate of groundwater flow through the potential repository site was dependent upon the hydraulic conductivity of the BVG, and was unaffected by the hydraulic conductivity of other hydrostratigraphic units. Calibration of the model was achieved by matching simulated subsurface pressures to those measured in situ. Simulations performed with BVG hydraulic conductivity 100 times the base case median value provided the "best-fit" comparison between the calculated equivalent freshwater head and that measured in situ, regardless of the hydraulic conductivity of other hydrostratigraphic units. Transient mass transport simulations utilising the hydraulic conductivities of this "best fit" simulation showed that fluids passing through the potential repository site could reach the surface in 15 000 years. Simple safety case implications drawn from the results of the study showed that the measured BVG hydraulic conductivity must be less than  $0.03 \text{ m year}^{-1}$  to be simply declared safe. Recent BVG hydraulic conductivity measurements showed that the maximum BVG hydraulic conductivity is around 1000 times this safety limit. © 1999 Elsevier Science B.V. All rights reserved.

*Keywords:* Finite element modelling; Groundwater flow; Radioactive waste

---

\* Corresponding author. Fax: +44-131-668-3184; e-mail: Stuart.Haszeldine@glg.ed.ac.uk

<sup>1</sup> Present address: Department of Petroleum Engineering, Heriot-Watt University, Edinburgh, EH14 4AS, Scotland.

<sup>2</sup> Present address: Department of Geology and Geophysics, University of Edinburgh, Edinburgh, EH9 3JW, Scotland.

**1. Introduction**

Britain’s first repository for intermediate level waste (ILW) was proposed to be situated 650 m below ground and 3 km to the east of the British Nuclear Fuels Ltd (BNFL) Sellafield fuel reprocessing plant (THORP) in West Cumbria, north-west England (Fig. 1). The repository was to utilise a system of multi-barrier containment, i.e. wastes were to be immobilised, packaged in concrete or stainless steel/mild steel containers, emplaced in repository vaults and back-filled with alkaline cement-based grout, with the final barrier being the geosphere itself. After 5 years of intensive site-specific investigation, the site has been rejected as unsuitable; partly due to the complexity of the

natural hydrogeology (McDonald et al., 1996). Technical and political issues are further reported in Couples et al. (1998) and Haszeldine and Smythe (1997). This experience teaches that when choosing a suitable repository site, the pattern and rate of underground water flow must be both predictable and safe for geologically long periods into the future (Chapman, 1994). Flow rates should be slow and flow paths preferably downward directed and of long distance, resulting in progressive mixing with older, deeper waters. Thus, a repository should be sited in an area with low regional hydraulic gradients (Chapman and McEwen, 1986). This paper presents results from a modelling study of the regional groundwater movement in the Sellafield area and utilises a 2D

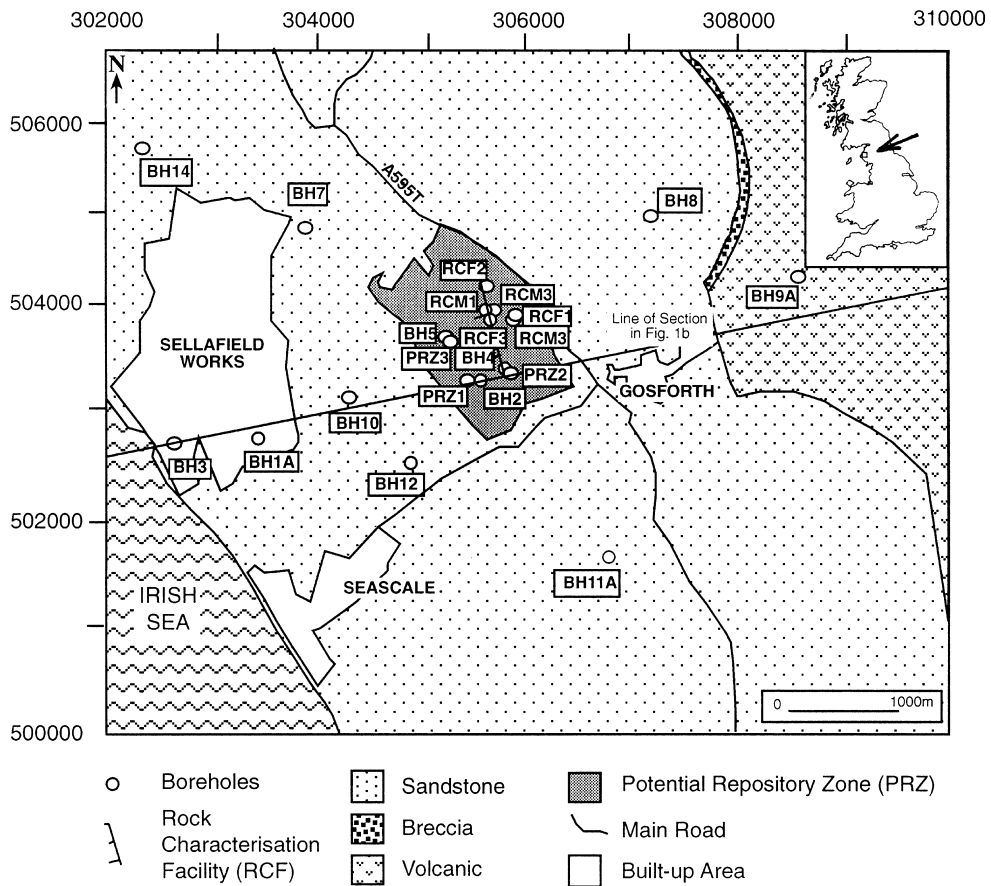


Fig. 1. Location of deep boreholes, line of geological cross section and the potential repository zone (PRZ) (after Michie and Bowden, 1994).

finite element fluid and heat flow code called OILGEN (Garven, 1989). The main aim of the paper is to develop geologically realistic numerical models where the relative importance of hydrogeological parameters can be scoped out. Sensitivity analysis was used to test the robustness of the conceptual model of the groundwater flow regime. This sensitivity analysis also allowed us to determine whether a particular rock type controls the movement of water through a potential repository. The simulator allows users to calculate vertical pressure profiles which were compared with those measured in situ. This allowed us to determine the “best fit” simulation by means of such comparisons, and then develop safety case assessments by utilising the tracking of fluid release pathways, and timescales in the simulations.

## 2. Geology and hydrogeology

The construction of fluid flow models requires good quality input data; the model is only as good as the information that is “fed in” to the computer simulation code. It is important to note that the authors did *not* gather such data; as the Sellafield site was a closed site, *all* data was collected by either UK Nirex Ltd or their sub-contractors from

around 1991 onwards. Airborne magnetic and gravity surveys were undertaken to complement existing data (Nirex, 1992a), offshore 2D and onshore 3D seismic data (Smythe, 1996) were collected as well as 2D geophysical tomographic surveys between pairs of boreholes. By 1995, there were a total of 22 continuously cored boreholes in the Sellafield area, with a total of 25 712 m of drilling (Chaplow, 1995). Information was derived (both from core and downhole logging) regarding geochemistry, rock mechanics, fracture geometry and hydrogeological data such as fluid pressure, permeability and porosity. (Michie and Bowden, 1994). Fig. 2 shows a geological cross-section through the Sellafield area running WSW–ENE through the potential repository zone (PRZ), passing through site investigation boreholes 3 and 2, and close to boreholes 1, 10 and 4. This section was based on information available at the start of the research project (Nirex, 1992a, 1993a,b) and has been extended both seaward and landward, using public geological and topographical information (Taylor et al., 1971). More detailed information has been published since our investigation commenced (Nirex, 1995b, 1997). However, the fundamental geology and hydrogeology remains unchanged.

The proposed repository site (Fig. 2) was at

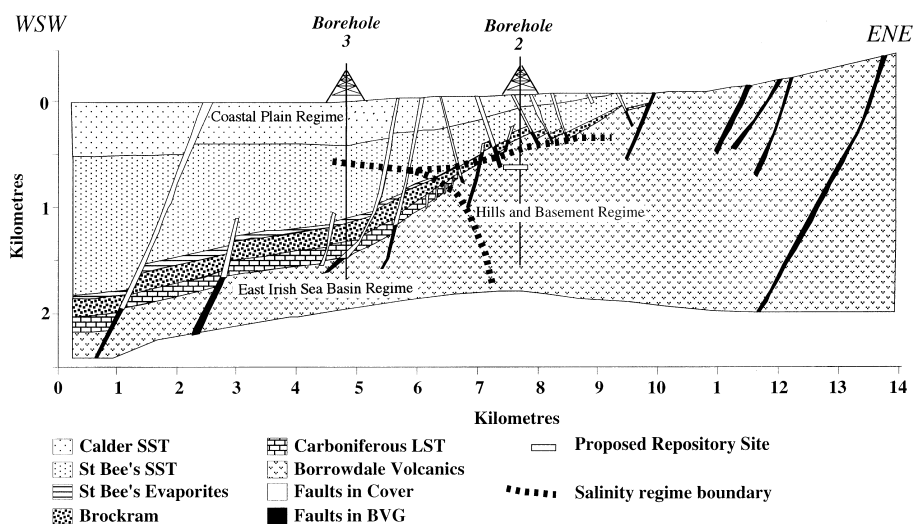


Fig. 2. Geological cross-section of the proposed repository site at 650 m, compiled from published information. Geological model is superimposed with conceptual model of the hydrogeology of the Sellafield area (after Black, 1995).

least 650 m below the subsurface within rocks of the Borrowdale volcanic group (BVG), a 2000–6000 m thickness (regionally) of heavily fractured and folded Ordovician meta-andesites and tuffs. The BVG also forms many of the hills in the upland areas to the east (Pettersen et al., 1992). The BVG is unconformably overlapped by 400 m of Carboniferous limestones, Permian clastics and evaporites and more than 1500 m of Triassic sandstones. The structural configuration of the post-Ordovician rock units is generally simple, with westerly dips of around 20° being typical (Michie, 1996). However, faults disrupt the continuity of the rock sequences and may be intimately involved in causing the westerly dips of the post-Ordovician strata. NW–SE trending faults dominate, dipping steeply towards the SW (Chadwick et al., 1994). The rock properties relevant to the hydrogeology of the region have been measured by Nirex (1993a) and can be simplified such that the Calder and St Bees sandstones are permeable and porous; the Brockram breccia and St Bees evaporites are impermeable and of low porosity; the Carboniferous limestone is slightly more permeable and the BVG is of low to medium permeability and low porosity (Table 1). The faults in both the cover and BVG are more permeable than the surrounding rock matrix with moderate porosity. A feature of these measurements is the wide range

of Calder sandstone hydraulic conductivity and the very wide range of BVG hydraulic conductivity ( $10^7$ ), and the narrower range of hydraulic conductivity in the overlying sediments. Consequently, there is uncertainty about which values represent regional hydraulic conductivities.

### 2.1. Conceptual model of hydrogeology and boundary conditions

Published conceptual models of the regional hydrogeology (Black, 1995) indicated that there may be three distinct fluid regimes in the subsurface (Fig. 2). These are the: hills and basement regime (topographically driven, relatively low flux, saline groundwater); Irish sea basin regime (relatively low flux, hypersaline brines) and coastal plain regime (topographically driven, high flux, fresh groundwaters). The proposed repository was to be situated within the so-called hills and basement regime groundwater, within which there is a salinity of around 2% by weight. In the case of the Sellafield area, the most important process that has been identified is gravity-driven groundwater flow, moving in a generally SW direction (Haszeldine and McKeown, 1995; Black and Brightman, 1996; Littleboy, 1996). As can be seen in Fig. 2, the eastern boundary of the cross-section corresponds to the maximum height encountered

Table 1

Hydrogeological parameters used in groundwater flow models. Surface temperature = 15°C, model base geothermal heat flux = 70 mW m<sup>-2</sup>

Unit	“Base case” hydraulic conductivity (K) (m year <sup>-1</sup> )	Modelled range of K (m year <sup>-1</sup> )	Anisotropy $K_h/K_v$	Porosity (%)	Storage co-efficient (m <sup>-1</sup> )	Thermal conductivity (Wm °C <sup>-1</sup> )	Dispersivity $\alpha$ (m)	Dispersivity $\alpha$ (m)
Calder sandstone	3	3, 30, 300	$1.00 \times 10^{+1}$	20	$1.00 \times 10^{-4}$	3.1	10.0	1.0
St Bees sandstone	1.5	1.5, 15, 150	$1.00 \times 10^{+1}$	10	$1.00 \times 10^{-4}$	3.1	1.0	0.1
St Bees evaporites	$1.60 \times 10^{-3}$	$1.00 \times 10^{-3}$ , $1.00 \times 10^{-1}$ , 1.00	$1.00 \times 10^{+2}$	1	$1.00 \times 10^{-6}$	4.0	1.0	0.1
Brockram breccia	$9.46 \times 10^{-4}$	$1.00 \times 10^{-3}$ , $1.00 \times 10^{-1}$ , 1.00	$1.00 \times 10^{+2}$	10	$1.00 \times 10^{-4}$	3.1	1.0	0.1
Carboniferous limestone	$1.50 \times 10^{-1}$	N/A	$5.00 \times 10^{+1}$	1	$1.00 \times 10^{-4}$	3.1	1.0	0.1
Borrowdale volcanic group (BVG)	$1.20 \times 10^{-2}$	$1.20 \times 10^{-5}$ , $1.20 \times 10^{-4}$ , $1.20 \times 10^{-3}$ , $1.20 \times 10^{-2}$ , $1.20 \times 10^{-1}$ , $1.20 \times 10^{+1}$	5.00	1	$1.00 \times 10^{-6}$	4.0	1.0	0.1
Faults in cover	3 <sup>a</sup>	0.3, 3, 30 <sup>a</sup>	1.00	5	$1.00 \times 10^{-4}$	3.1	1.0	0.1
Faults in BVG	0.03 <sup>a</sup>	0.0003, 0.03, 3 <sup>a</sup>	1.00	2	$1.00 \times 10^{-4}$	3.1	1.0	0.1

<sup>a</sup> Modelled fault hydraulic conductivity. Equivalent to “real world” hydraulic conductivities that are 100 times greater (see Section 6 for details).

in the area; very little is known about flows in these outcropping basement rocks; thus it is appropriate when constructing a fluid flow model to assign a no-flow boundary to the eastern vertical edge. A similar situation regarding data applies to the flows west of the coast and, due to the highly saline nature of these fluids [21% by weight, possibly becoming more saline further offshore (Nirex, 1995b)], it is appropriate to assign a no-flow boundary to the western edge also. This highly saline groundwater is likely to persist at greater depths than those attained in the present boreholes (which are up to 2 km). At depths beyond the bottom hole, such highly saline, dense groundwater is likely to be relatively immobile, so again it is appropriate to assign a no-flow boundary to the base of the section. In modelling studies of groundwater flow, it is common to assume that the water table is coincident with the land surface and that water at this boundary would be fresh, thus it is acceptable to assign a boundary to the top surface that allows flow to pass through it.

### 3. Mathematical model

The vertical section shown in Fig. 2 was discretised exactly (Fig. 3) and used as the mathematical model of the regional flow system. In fractured rock (e.g. the BVG) the interconnected fractures

are the main passages for fluid flow, with the matrix being almost impermeable. This results in wide ranges of hydraulic conductivity, with fracture conductivity orders of magnitude greater than the matrix (Neumann, 1990; Clauser, 1992). Modelling flow in such a fractured system is problematic but can be achieved by: *either* modelling the fluid transport through each fracture or network of discrete fractures (Moreno and Neretnieks, 1993); *or* modelling the transport regime in the fractured mass as an equivalent porous and anisotropic continuum (Follin and Thunkin, 1994). If the spacing of fractures zones is less than the scale of numerical discretisation in the model, then the equivalent porous media approach is justifiable (Garven, 1994). It is the porous medium approach which has been adopted in this study.

### 4. Mathematical formulation

In models of regional groundwater flow, it is common to treat the continuum model as steady-state. The equation for the conservation of mass for steady state flow of a single phase fluid of density  $\rho$  is written as:

$$\nabla \times (\rho \mathbf{q}) = 0 \quad (1)$$

where  $\mathbf{q}$  is the specific discharge vector (often

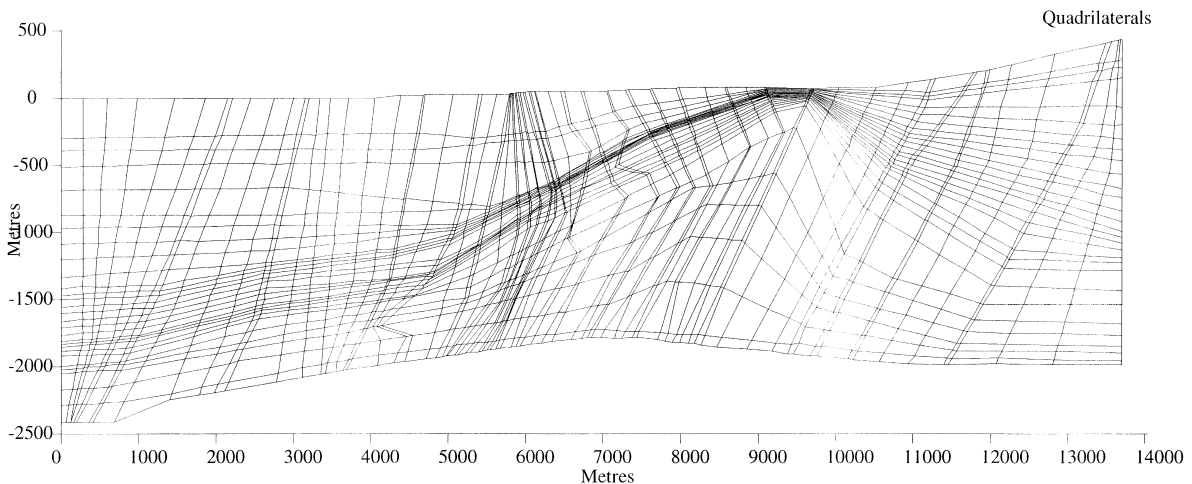


Fig. 3. Finite element model derived from Fig. 2 used to simulate single phase fluid flow. See text for boundary conditions.

termed the Darcy velocity), commonly presented in  $\text{ms}^{-1}$  and  $\nabla$  is the differential operation, defined by:

$$\nabla = \frac{\partial}{\partial x} \mathbf{i} + \frac{\partial}{\partial z} \mathbf{k} \quad (2)$$

where  $\mathbf{i}$  and  $\mathbf{k}$  are the unit vectors in the  $x$  and  $z$  directions. The specific discharge vector  $\mathbf{q}$  is given by the general term of Darcy's Law:

$$\mathbf{q} = -\frac{\mathbf{k}}{\mu} (\nabla p + \rho g \nabla Z) \quad (3)$$

where  $\mathbf{k}$  is the permeability tensor,  $\mu$  is the ambient fluid viscosity,  $p$  is fluid pressure,  $g$  is gravitational acceleration and  $Z$  is the elevation. Since groundwaters often differ in density, it is necessary to define relative viscosity,  $\mu_r = \mu/\mu_0$ , and the relative fluid density,  $\rho_r = (\rho_0 - \rho)/\rho_0$ , where  $\mu_0$  is the reference state viscosity, defined at the same temperature, pressure and salinity as the reference state density,  $\rho_0$ . The model utilises the concept of equivalent fresh-water head,  $h$  (Bear, 1972):

$$h = \frac{p}{\rho_0 g} + Z \quad (4)$$

If the permeability tensor  $\mathbf{k}$  is replaced by the hydraulic conductivity tensor  $\mathbf{K}$ , where:

$$\mathbf{K} = \frac{\mathbf{k} \rho_0 g}{\mu_0} \quad (5)$$

then Eq. (3) can be modified for groundwater of variable density:

$$\mathbf{q} = -\mathbf{K} \mu_r (\nabla h + \rho_r \nabla Z) = v \phi \quad (6)$$

where  $v$  is the average linear velocity or seepage velocity and  $\phi$  is porosity. At steady-state, the conservation of thermal energy can be expressed as:

$$\nabla \cdot [\mathbf{E} \nabla T] - \rho c \mathbf{q} \cdot \nabla T = 0 \quad (7)$$

where  $\mathbf{E}$  is the combined thermal conductivity–dispersion tensor (derived from the thermal conductivity, porosity and thermal dispersion of the material),  $c$  is the specific heat capacity of water and  $T$  is temperature. The transport of mass is a transient phenomenon, thus Eq. (1) can no longer

be dealt with as steady-state and a new term has to be introduced to the right-hand side:

$$-\nabla \cdot (\rho \mathbf{q}) = \rho S_s \frac{\partial h}{\partial t} \quad (8)$$

where  $S_s$  is the specific storage coefficient; defined as the volume of water released from a unit volume of rock for a unit decline in head (units of  $\text{m}^{-1}$ ), and  $t$  is time.

#### 4.1. Numerical formulation and solution procedure

The irregular geometry of the Sellafield area makes the finite element technique most suitable for solving the flow equations above (Kazda, 1990). Fig. 3 shows the finite element grid of quadrilaterals used in this modelling study. Each element is composed of a material that may have distinct rock properties such as porosity and permeability. Boundaries within the mesh have no special qualities; flow crosses between elements of different porosity and hydraulic conductivity. Flow rates are constant over individual elements, but discontinuous across element boundaries. A spatially variable fluid salinity profile (based on field data) can be assigned to the grid, however the code does not allow a fully coupled density–flow solution. The governing equations are approximated by matrix equations via a standard Galerkin finite element procedure (Huyakorn and Pinder, 1983). Once the prescribed boundary conditions are included, the code utilises the Galerkin weighted average formulation (de Marsily, 1986) to solve the flow equation to calculate the steady-state hydraulic head distribution. The Darcy velocities in each triangular element (i.e. subdivisions of the quadrilaterals) are then calculated for each node Eq. (6).

The steady state heat equation [Eq. (7)] is then solved to determine the temperature variation in the grid; these new values of pressure, temperature and salinity profile are used to calculate fluid densities and viscosities from the equations of state (Kestin et al., 1981). The code then iterates these steps until convergence of temperature change reaches less than  $1^\circ\text{C}$ . Although the variable salinity profile is fixed in space and time, the density

and viscosity of the grid may not be. Once the steady-state velocity distribution is calculated and the equation of conservation of fluid mass observed, mass transport is simulated using a moving-particle random-walk method (LaBolle et al., 1996). During a prescribed time step, each particle is advected according to the magnitude of average linear velocity of the fluid in the element, with hydrodynamic dispersion simulated by the displacement of the particle position using the random walk method. The displacement is calculated from an expression relating the assigned longitudinal and transverse dispersion coefficients, time steps and a randomly generated number in the range 0–1 (Garven, 1989). These particles have the same density and temperature as the surrounding water, so that they are passive indicators of water flow paths and dispersion, and do not have any inherent buoyancy or capillarity effects.

## 5. Modelling method

OILGEN requires a fixed number of hydrostratigraphic units (Table 1). The hydrostratigraphic units are defined fundamentally on the basis of their porosity,  $\phi$  (expressed as a percentage), and hydraulic conductivity,  $K$  ( $\text{m year}^{-1}$ ). Values for these were derived from published data (Nirex, 1992a, 1993a; Michie, 1996) and for the purpose of this study have been simplified to ignore any variations in conductivity due to water salinity. The values reported are close to logarithmic median values of hydraulic conductivity. These will be termed the “base case” values in this modelling study and are used as the basis for extended modelling over a range of hydraulic conductivity values. The geothermal heat flux at the base of all the models was constrained at  $70 \text{ mW m}^{-2}$  with the temperature at the water table of  $15^\circ\text{C}$ . The storage coefficients ( $m^{-1}$ ) of confined rocks can vary by as much as three orders of magnitude up to  $10^{-3}$  and values used in this study were similar to those published elsewhere (Garven, 1989). The thermal conductivities of most rocks lie in the range  $1\text{--}8 \text{ W m}^{-1} \text{ }^\circ\text{C}^{-1}$ . (Raffensperger and Garven, 1995) with many compilations of such data published in the literature

(Andrews-Speed et al., 1984; Deming et al., 1992). Coefficients of lateral and longitudinal dispersion are based on published material.

The sensitivity analysis approach was utilised in this study (Lerche, 1990); before each simulation, a numerical attribute of the model was varied and the code run to completion. If the result did not change significantly from the previous experiment then that particular attribute was deemed unimportant. If the result did change, then it would be vital to measure that attribute as accurately as possible in the actual geological setting. At this site, there are good data on rock stratigraphy and geometry. However, it is known from borehole data that the BVG has a fracture hydraulic conductivity some  $10^2$  greater than matrix conductivity (Nirex, 1992a, 1993b), as do most crystalline rocks (Brace, 1980; Clauser, 1992). Borehole measurements indicate that fluid flow in the BVG is controlled by fractures, which have a spacing of 50–100 m (at least one fracture per finite element). Thus, this can be treated as a matrix conductivity, (Follin and Thunkin, 1994).

## 6. Simulation results

The results presented in this paper are an abridged version of the results from all the simulations performed (McKeown, 1997). It is the aim of this section to briefly explain the approach taken and summarise results from simplistic and scoping modelling before presenting, in more detail, the results from the sensitivity modelling study that was most pertinent to a safety case assessment of the hydrogeology of the Sellafield area. For the fluid flow simulations, the groundwater flow rates and directions are depicted by arrows representing the vector of the average linear velocity [from Eq. (6)] of fluid within a particular element. The tail of the vector is located in the centre of the relevant element. Each vector is scaled relative to the length of the arrow shown at the top of each plot. An element of standardisation has been applied in that, for the sake of comparison between plots, the arrows are scaled to either 2, 20 or  $200 \text{ m year}^{-1}$ .

Crosses indicate that flow is less than 1% of the

maximum for that plot, so that water could still be moving, but relatively slowly. OILGEN calculates the hydraulic head distribution taking into account the variation in density, temperature and viscosity. However, in the grid, OILGEN plots hydraulic head as equivalent freshwater head, i.e. the height above ground that surface *fresh* water would rise to under the pressure at the specified depth. Plots of equivalent freshwater hydraulic head are contoured from the ordnance datum (OD), i.e. sea level, and have contours spaced at 20 m intervals. Contours of equivalent freshwater hydraulic heads join areas of equal potential in a flow system. Water can flow from high to low potential given a suitable route, i.e. flow perpendicular to contours.

An important parameter when modelling groundwater flow in faults is transmissivity ( $T$ ), defined, most simply when hydraulic conductivity ( $K$ ) is isotropic, as:

$$T = Ke \quad (9)$$

where  $e$  is the width of the fault aperture (de Marsily, 1986). This relationship was used when modelling the effect of faults in the simulations. Faults were treated by modelling artificially wide quadrilaterals, but with correspondingly reduced hydraulic conductivity. Consequently, as faults were isotropic in all simulations, the “effective” transmissivity is as it should be. For example, a real fault 1 m wide, 30 m year<sup>-1</sup> hydraulic conductivity, is modelled as 100 m wide, 0.3 m year<sup>-1</sup> hydraulic conductivity.

Preliminary simulations performed in the early stages of this study and previously published (Haszeldine and McKeown, 1995; McKeown and Haszeldine, 1995), utilised values of hydraulic conductivity for faults in the sediments and BVG of 300 and 1 m year<sup>-1</sup>, respectively. Recently published data indicated that a revision of these values was necessary (Michie, 1996). The 300 m year<sup>-1</sup> value for the faults in the sediments was derived as a log mean of published EPM and pumping tests (Nirex, 1993a). The inclusion of pump test values in “base case” models may be spurious as only very productive faults were sampled (Nicholls, 1995). Therefore, a high value for the faults in sediments may not be representative of

the average hydraulic conductivity of the majority of the faults. The measured hydraulic conductivity values (Table 1) used as “base case” for faults in the sediments and BVG, of 30 and 3 m year<sup>-1</sup>, respectively, are similar to values reported in other modelling studies (Nicholls, 1995; Nirex, 1995b; Heathcote et al., 1996). The faults in the OILGEN model are, in general, some 100 times wider than those observed in the field (Nirex, 1993a) and a “base case” was represented in these simulations by modelling faults as isotropic units with  $K=0.3$  and 0.03 m year<sup>-1</sup> for faults in the cover and BVG, respectively.

### 6.1. Simplistic models

Before performing sensitivity analysis on the geologically complex model, shown in Fig. 3, simulations were performed upon a very simple model (Fig. 4) that had the same boundary conditions, fluid properties, lateral extent, thickness, number of cells and hydrostratigraphic parameters as the more complex models. This “simplistic” modelling was used to develop an understanding of the fluid flow system that may be encountered, given the prescribed boundary conditions, hydraulic parameters, density of fluids and the spatial relationships of the hydrostratigraphic units. Simplistic modelling also provided a comparison with the more complex grid to delineate if the pattern and rate of fluid flow were affected by the orientation, size and shape of the grid cells. Plots of average linear velocity (Fig. 5) showed that, for models populated with BVG, cover sediments and evaporites and breccias, there is a regional flow pathway of “diagonal” transfer of topographically driven groundwater into sediments. There is an upward trending deflection of groundwater flow in the BVG in the central areas of the model. This corresponds to the location of a possible repository in the more realistic model. Thus the regional flow pattern is considered to be a fundamental feature of the study area, and is not influenced by any artefacts of model gridding, or complexities of geology. The dominant control on upwards flow from the BVG to the sediment is the dense, immobile saline water in the western edge of the model.

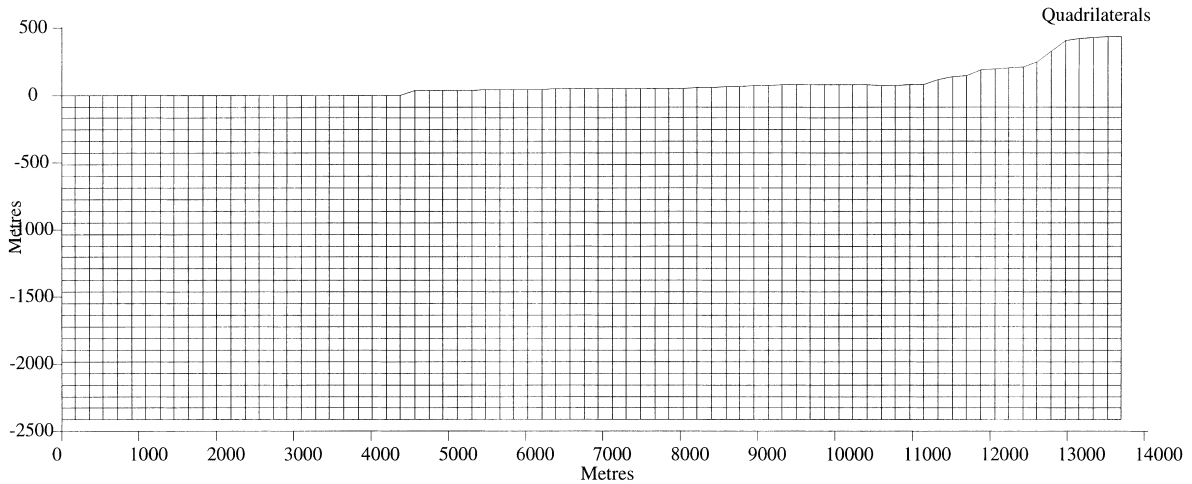


Fig. 4. Uniform grid used in simplistic simulations. See text for boundary conditions.

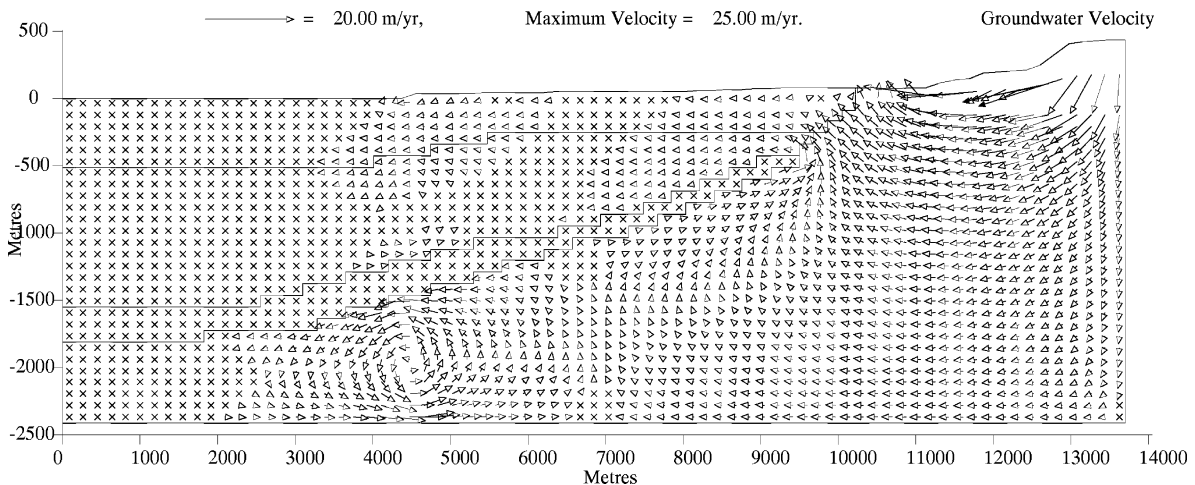


Fig. 5. Average linear velocities calculated with a simple grid, with variable salinity profile, and hydraulic conductivities set to “base-case” (Table 1), except BVG ( $1.2 \text{ m year}^{-1}$ ).

### 6.2. Importance of faults, salinity and BVG anisotropy

A scoping study was performed to find whether: (a) the presence or absence of faults, and a variable salinity profile; and (b) variations in BVG anisotropy, were important in the simulations. Comparisons can be made of the calculated head to the subsurface head observed in boreholes from the Sellafield area. Fig. 6 is a west–east cross-section showing contoured variations in the fresh-

water head measured in the field. It was found that the freshwater head contours determined from pressures measured in the field are markedly different from those of the model without faults. It was found that, in order to obtain a similar hydraulic head profile to that contoured from field data, it was essential that: (a) the models included a variable salinity fluid; and (b) faults had to be incorporated. Fig. 7 shows an equivalent freshwater head calculated with “base case” hydro parameters (Table 1), apart from the BVG hydro-

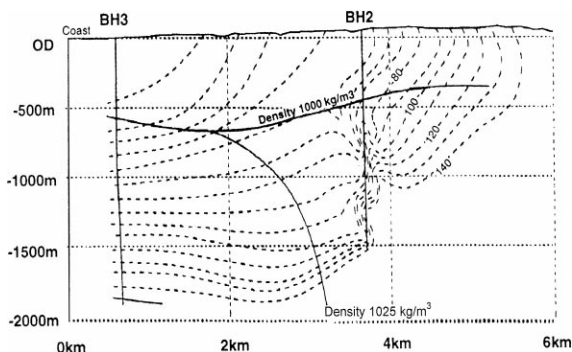


Fig. 6. West–east cross-section showing variations in freshwater head measured in the field (after Black and Brightman, 1996).

lic conductivity, which is set to  $1.2 \text{ m year}^{-1}$ . Fig. 7 illustrates the similarity of the head gradients to those measured in the field (Fig. 6) and also displays some features that were common to all of the more complex models. There is evidence for the potential for topographically driven flow in the BVG, with potential for diagonal flow in the central region and high vertical gradients in the western area of 16% salinity. The general flow pattern (as illustrated in Fig. 8, which has the same hydro parameters as the model shown in Fig. 7) is extremely robust i.e. topographically driven groundwater descending, advecting to the west, traversing low permeability units via faults and generally moving upwards to surface. This is

assisted by deflection eddies, caused by density-induced flows from areas of high salinity. Lateral movement of fluids in sediments has little effect on the flow regime.

The similarity of results from the simple (Fig. 5) and more complex models (Fig. 8) indicates that the shape and size of the finite element cells is not relevant to either the flow rate or the flow path, nor indeed to the numerical solution of the flow and heat transport equations. This gives confidence in the OILGEN code. It was found that varying the anisotropy of the BVG had very little effect on the calculated flow rate through a potential repository. This suggests that the direction and rate of flow in the BVG is not controlled by the shape of the finite element cells, and that the cross-sectional area of the BVG is so large that fracture orientation may have little importance in the real world.

## 7. Sensitivity analyses of Calder sandstone and BVG permeability ranges

As outlined earlier, the original data used in the early stages of this study indicated that only two hydrostratigraphic units, the Calder sandstone and the BVG, had substantial ranges in hydraulic conductivity. These two units are significant to the

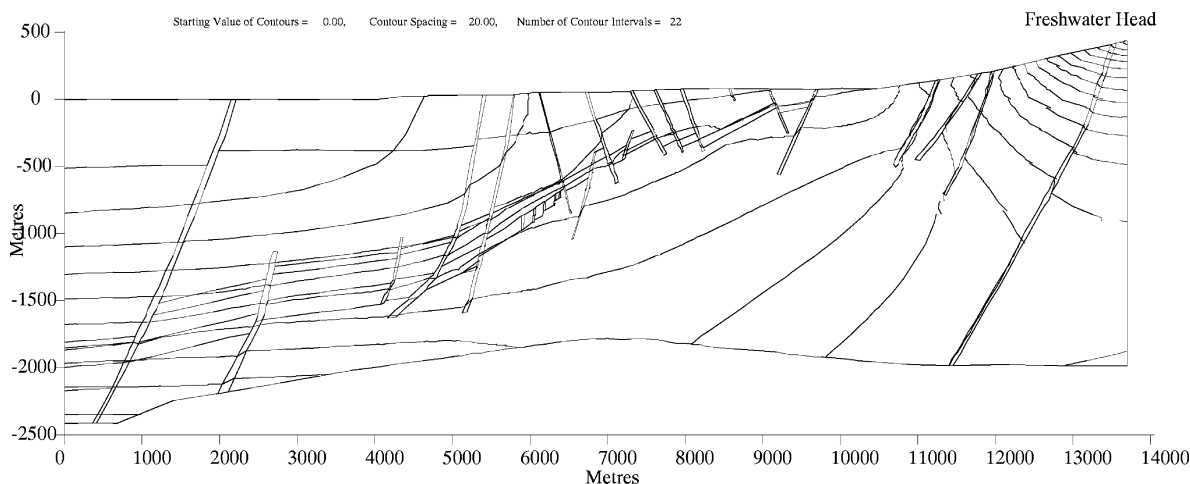


Fig. 7. Contoured equivalent freshwater head calculated with a complex model (Fig. 3). Model has faults and variable salinity profile. Hydraulic conductivities set to “base-case” (Table 1), except BVG ( $1.2 \text{ m year}^{-1}$ ).

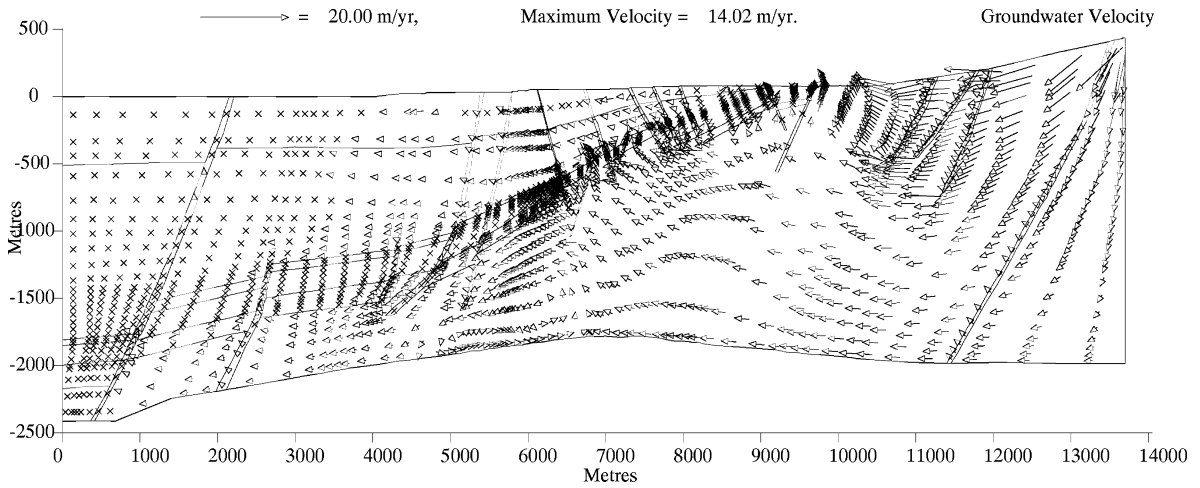


Fig. 8. Average linear velocities calculated with a complex model (Fig. 3). Model has faults and variable salinity profile. Hydraulic conductivities set to “base-case” (Table 1), except BVG ( $1.2 \text{ m year}^{-1}$ ).

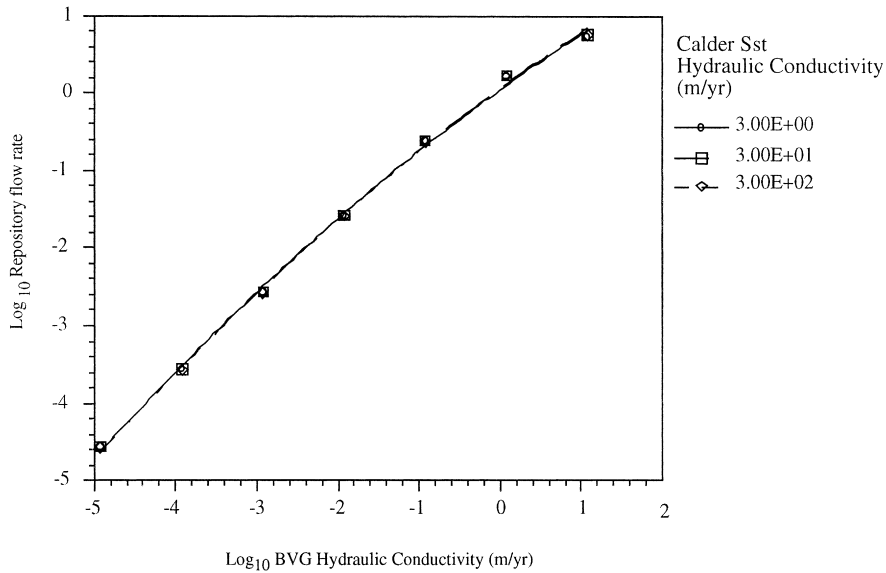


Fig. 9. Log–log plot of repository flow rate versus BVG hydraulic conductivity. Results from varying Calder sandstone hydraulic conductivity superimposed.

geological and radiological problem. The BVG needs to have low flow to retain radionuclides in the repository. The Calder sandstone, being a rapidly flowing freshwater aquifer, also plays a role in the safety case of the repository. The rapid flows have the possibility of diluting and dispersing any release of radionuclides. To this end, these two units were modelled to investigate the range

of hydraulic conductivities shown in Table 1. The Calder sandstone (CS) was modelled with hydraulic conductivity of 3, 30 and  $300 \text{ m year}^{-1}$  for the entire range of BVG hydraulic conductivity of  $1.20 \times 10^{-5}$  to  $1.20 \times 10^{+1} \text{ m year}^{-1}$ . The BVG hydraulic conductivity of  $1.2 \text{ m year}^{-1}$  used in previous parts of this study is still somewhat less than the maximum measured in the field in the

Sellafield area, (Nirex, 1993a; Michie, 1996). Therefore, the modelled range was extended to  $12 \text{ m year}^{-1}$ .

The OILGEN code produces numerical values that can be interrogated for particular nodes or elements of the mesh and thus the velocity of groundwater through the element that relates to the position of a putative repository can be extracted. Fig. 9 summarises the results of 21 simulations with a seven order of magnitude range in BVG hydraulic conductivity, and each model run with Calder sandstone hydraulic conductivity of either 3, 30 and  $300 \text{ m year}^{-1}$ . In these 21 experiments, flow rate through the repository is directly related to BVG hydraulic conductivity regardless of the Calder sandstone hydraulic conductivity. The pattern of flow direction remains similar in all cases, with upward flow at the 650–1000 m BOD depth proposed for the repository.

In a (fictional) homogenous system, Darcy's law shows that the velocity of fluid through a porous medium should be linearly related to the permeability (given that other parameters remain constant). However, there may be no simple relationship between permeability and flow in a complex system within which there are considerable spatial differences in material properties. Surprisingly, there are simple, log-linear relationships present in the simulations reported above. The fluid velocity through the BVG element representing the repository is extremely dependent upon the hydraulic conductivity of the BVG but independent of the hydraulic conductivity of the Calder sandstone. As these two hydrogeological units may be significant elements of the regional flow system, the observed relationship indicates that these units are hydrologically de-coupled. That is, their circulation patterns are controlled by essentially separate influx/outflux sites and their driving energies are separate. The only contribution of the Calder sandstone aquifer to the repository safety is the possible seaward transport, dilution and dispersion of any waters and radionuclides migrating upwards from the repository through the BVG. The pattern of flow through the repository is persistently upwards, through several decade values of BVG conductivity experiments. These flow patterns imply that water from the repository could eventu-

ally reach the surface as springs in the BVG outcrop, or by dispersion within the Calder sandstone. Hence, the proposed repository position would need to engineer against natural groundwater flow, rather than be assisted by it.

### 7.1. Sensitivity of other variables

As already mentioned, the original modelling performed for this study was undertaken with the expectation that the CS and BVG would have the widest range in values of hydraulic conductivity. In order to scope out the effects of variations in other units, simulations were performed where:

- St Bees sandstone hydraulic conductivity was varied over the range 1.5, 15 and  $150 \text{ m year}^{-1}$ .
- Faults in the cover sequence were varied over the range 0.3, 3 and  $30 \text{ m year}^{-1}$  (as mentioned above, these over-wide faults simulate "real world" faults with actual hydraulic conductivities of 30, 300 and  $3000 \text{ m year}^{-1}$ ).
- Faults in the BVG were varied over the range  $3.00 \times 10^{-4}$ ,  $3.00 \times 10^{-2}$  and  $3.00 \text{ m year}^{-1}$  (as above, simulating "real world" faults of 0.03, 3 and  $300 \text{ m year}^{-1}$ ).
- The low permeability of St Bees evaporites and Brockram breccia were modelled over the range  $1.50 \times 10^{-3}$ ,  $1.50 \times 10^{-1}$  and  $1.50 \text{ m year}^{-1}$ .

Fig. 10 shows that varying the St Bees sandstone hydraulic conductivity for the entire range of BVG hydraulic conductivity has no effect on the flow rate through the repository. Thus the St Bees sandstone is unimportant with regard to flow rates but could still contribute to containing radionuclide leakage by dispersion and dilution, but this is uncertain and minor. In order to model the effect of varying the hydraulic conductivity of the cover faults, BVG faults, St Bees evaporites and Brockram breccia, the simulation where BVG hydraulic conductivity was set to  $1.2 \text{ m year}^{-1}$  was run for the range of values outlined above. As can be seen in Table 2, the variation of these attributes had very little effect on the flow rate through the repository and can be thought of as unimportant as regards flow rates.

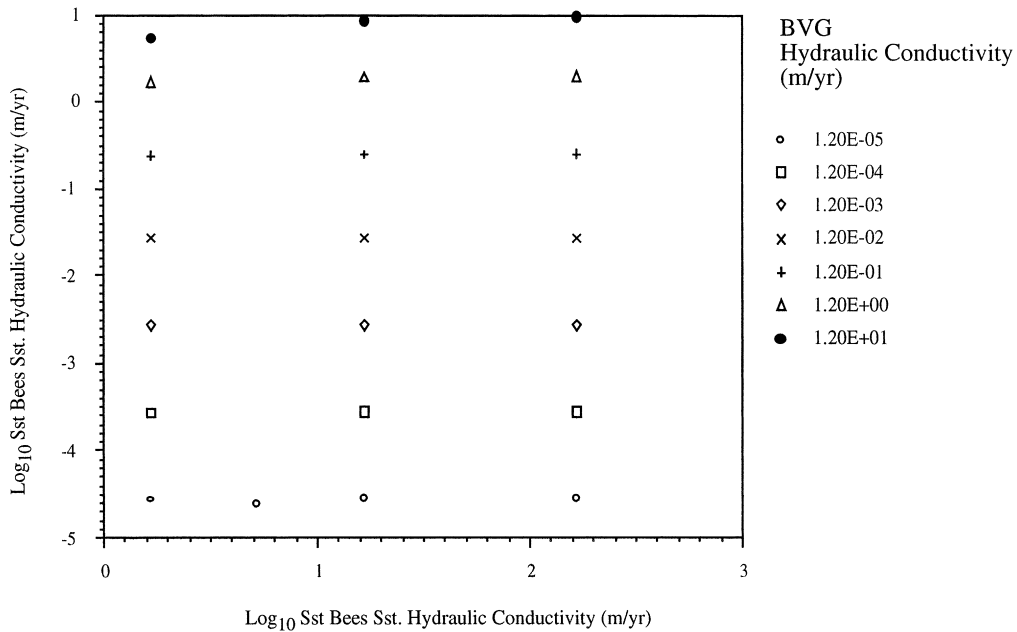


Fig. 10. Log–log plot of repository flow rate versus St Bees sandstone hydraulic conductivity. Results from varying BVG hydraulic conductivity superimposed.

Table 2

Calculated flow velocity through potential repository for range in hydraulic conductivity of: BVG faults; cover faults and St Bees evaporites/Brockram breccia

Input BVG faults $K$ (m year <sup>-1</sup> )	Result Repository flow rate (m year <sup>-1</sup> )	Input Cover faults $K$ (m year <sup>-1</sup> )	Result Repository flow rate (m year <sup>-1</sup> )	Input Evaporites + Brockram $K$ (m year <sup>-1</sup> )	Result Repository flow rate (m year <sup>-1</sup> )
$3.00 \times 10^{-4}$	1.47	0.3	1.68	$1.50 \times 10^{-3}$	1.68
$3.00 \times 10^{-2}$	1.68	3.0	2.00	$1.50 \times 10^{-1}$	1.72
3.00	2.06	30.0	2.44	1.50	1.82

### 8. Comparison of calculated and measured freshwater hydraulic head

It has been maintained elsewhere (Black and Brightman, 1996; Heathcote et al., 1996) that if there is a spatially varying solution density in either the vertical or horizontal plane, no information on the potential for flow in the 1D vertical plane can be derived from vertical plots of the freshwater hydraulic head and the use of an environmental head is required (Luszczynski, 1961; Bachu, 1994). However, the freshwater head is calculated from the pressure measured in situ and

is therefore a true representation of the hydraulic head at a given point in the subsurface, i.e. the height above the ground that surface freshwater would rise to if a route was available. Although OILGEN calculates head, taking into account variations in temperature, viscosity and more importantly density, it represents head as equivalent freshwater head. It is instructive to perform a comparison between the calculated equivalent freshwater head and the observed freshwater head in boreholes of the Sellafield area. This acts as a validation exercise for the realism of the model. No information regarding vertical head gradients

is inferred from these comparisons. The position of boreholes 2 and 3 are shown in the cross-section used as the basis for the complex grid. The OILGEN code can generate an output file that has equivalent freshwater hydraulic head values in any chosen vertical 1D section.

### 8.1. Measured head plots

The observed freshwater head plots (black squares in Figs. 11 and 12) were derived from published data (Nirex, 1992b) and represent spot results from environmental pressure measurement (EPM) tests. Note that the head values have been portrayed with respect to ordnance datum (OD). This takes into account the land topography vertically above the borehole. Dealing with the measured freshwater hydraulic head in borehole 2 first (Fig. 11), it is apparent that there is a distinct increase in head with depth, with a maximum of around 150 m at the base of borehole 2. The step-wise increase in head, punctuated at 350 and 600 m bOD is interrupted by a distinct drop in head between 800 and 1200 m bOD. Borehole 3 (Fig. 12) has a generally low head (<50 m) down to 800 m bOD, below this depth the head increases to a maximum of around 150 m at the bottom hole. Modelling must attempt to match these variations in the depth zone of interest, down to 700 m bOD.

### 8.2. Varying the BVG hydraulic conductivity

It has been illustrated that the BVG is the most important unit in the modelling simulations. Head comparisons were performed for boreholes 2 and 3, where all the units are set to their base case values and the BVG is varied from the base case value of  $0.012 \text{ m year}^{-1}$ , to 0.12 and  $1.2 \text{ m year}^{-1}$  (Fig. 11). There is a step-wise component in the head increase in borehole 2. None of the simulations could match the variation in head between 800 and 1200 m bOD. However, it has been reported that the BVG rock lithologies become more heterogeneous below 800 m bOD (Nirex, 1993a) and since the BVG was treated as a homogenous material in this study, it is unlikely that a good fit throughout will be made to the

measured head. The important zones are 0–700 m and the average trend continued to 1150–1500 m. As the target depth of the repository is 650 m bOD, it is significant that the simulation with the BVG hydraulic conductivity set at  $1.2 \text{ m year}^{-1}$  has the best match to the observed head in borehole 2 down to 700 m bOD. This simulation also provides a fair, but not perfect, match to the deeper head data; 1150–1500 m. Other modelling studies of groundwater flow in the Sellafield area (Nirex, 1993a,b, 1995a; Nicholls, 1995; Heathcote et al., 1996) have been unable to reproduce the relatively high heads at depth in the BVG. The same range in BVG hydraulic conductivities are used to compare equivalent freshwater hydraulic head calculated from the model and head measured in situ in borehole 3 (Fig. 12). There is little difference between the simulations down to 750 m bOD, but the better fit at depth is again for the simulation where the BVG is set to  $1.2 \text{ m year}^{-1}$ .

### 8.3. St Bees evaporites and Brockram breccia and faults in the cover and BVG

Simulations were performed to test if variations in the hydraulic conductivity of the St Bees evaporites, Brockram breccia and faults in the cover and BVG had an effect on comparisons between observed head in boreholes 2 and 3 and that calculated with the model [see McKeown (1997) for more details]. Comparisons were made where the BVG is set to  $1.2 \text{ m year}^{-1}$  and the other units set to their base case values before variations were made in their hydraulic conductivity. The hydraulic conductivity of the St Bees evaporites and Brockram breccia was not found to greatly affect the head calibration. Faults in the BVG were varied over the range  $3.00 \times 10^{-4}$ ,  $3.00 \times 10^{-2}$  and  $3.00 \text{ m year}^{-1}$ . As outlined above, this simulates “real world” faults with hydraulic conductivity of as much as  $300 \text{ m year}^{-1}$ . As this is more than an order of magnitude greater than fault permeabilities used in similar studies (Nicholls, 1995) it is interesting to note that such a variation has a negligible affect on the calculated head in both boreholes 2 and 3. Thus, the permeability of the faults in the BVG has no major effect on the head

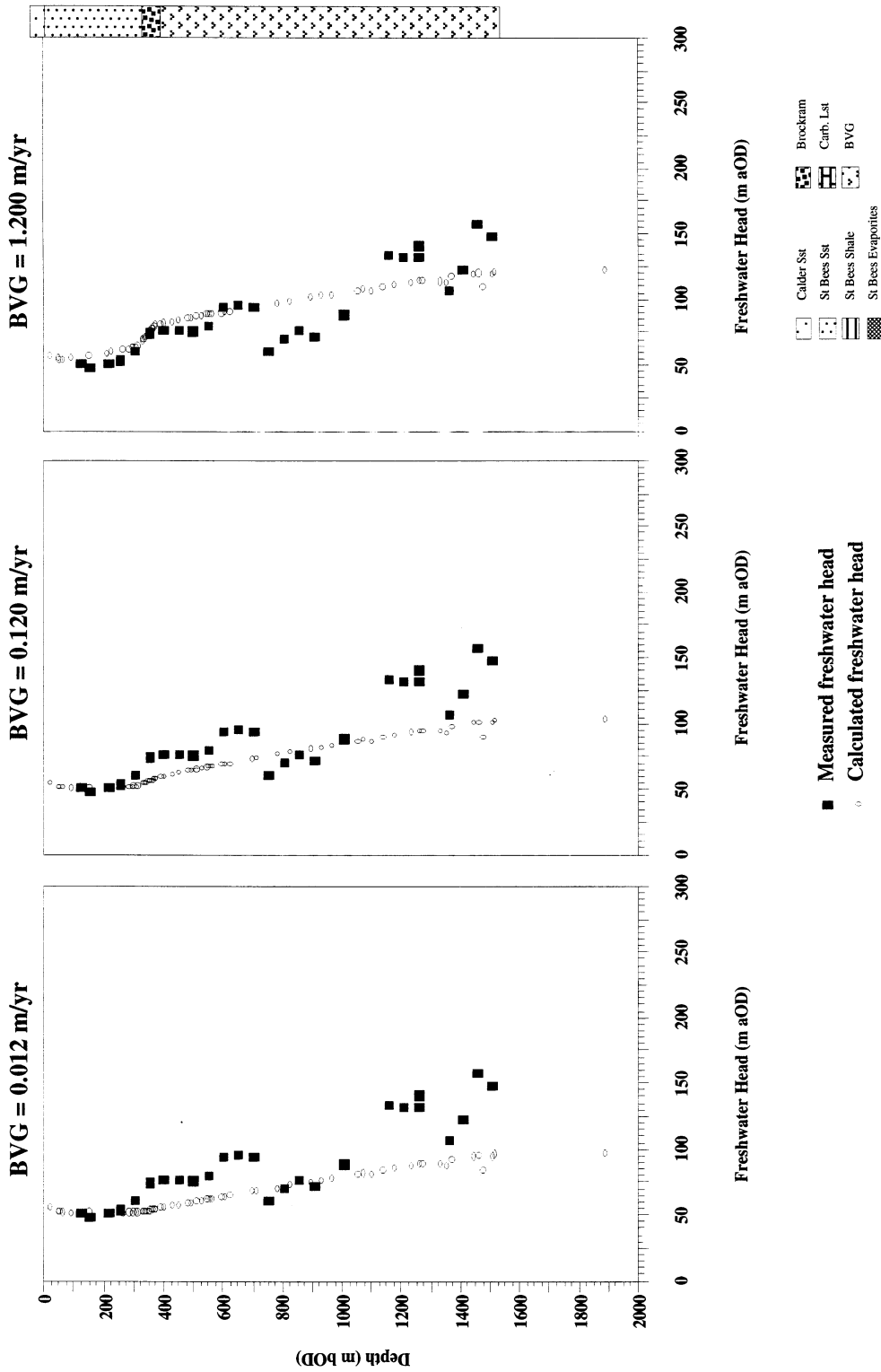


Fig. 11. Comparison of measured and calculated freshwater head in borehole 2. All parameters as those of “base-case” (Table 1), except BVG hydraulic conductivity ( $1.2 \times 10^{-2}$  to 1.2).

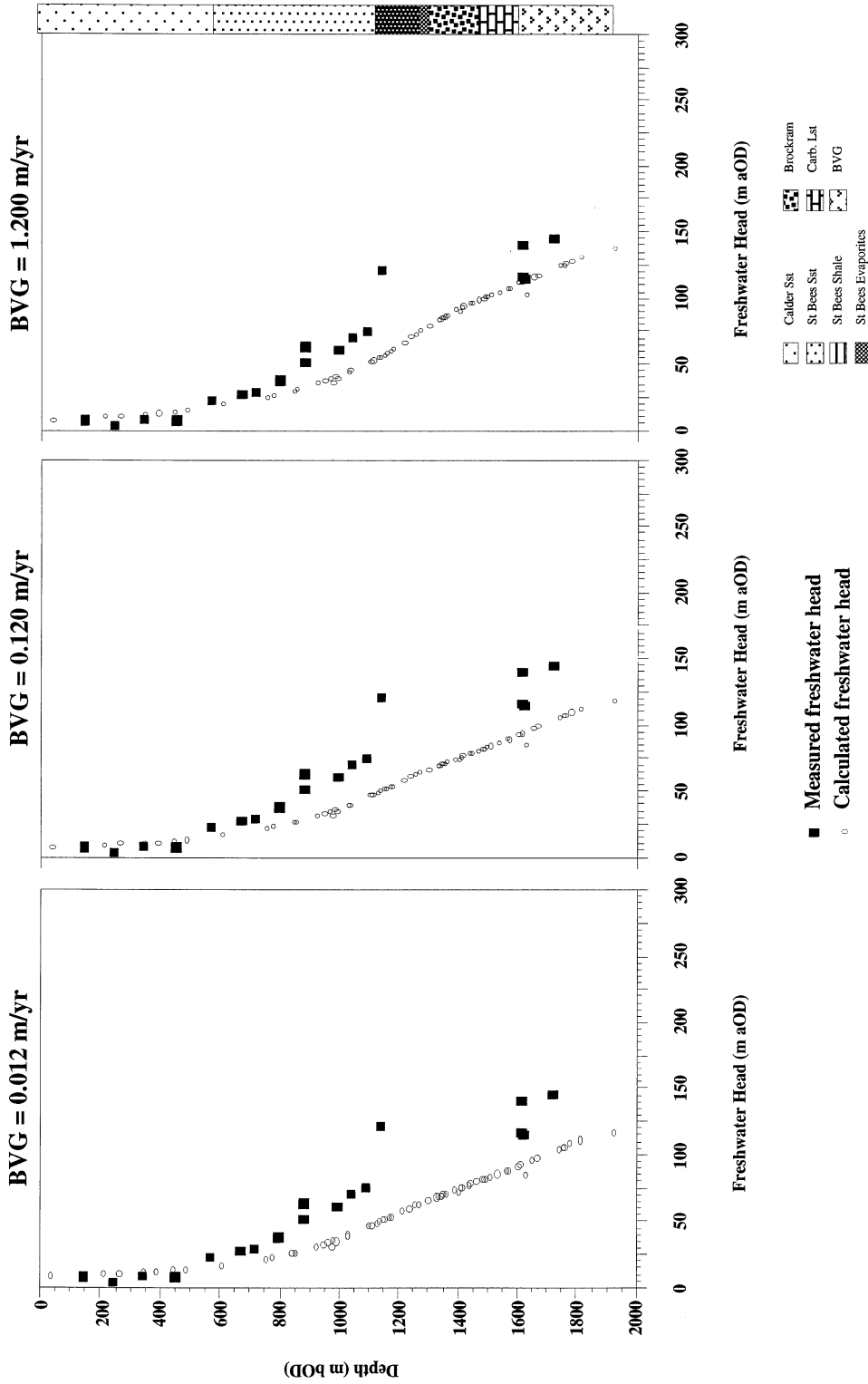


Fig. 12. Comparison of measured and calculated freshwater head in borehole 3. All parameters as those of “base-case” (Table 1), except BVG hydraulic conductivity ( $1.2 \times 10^{-2}$  to 1.2).

calibration. Varying the hydraulic conductivity of the cover faults over the range 0.3, 3 and 30 m year<sup>-1</sup> does have an effect on the match between freshwater head measured in situ and that calculated from the model. The comparison of the in situ freshwater head with that calculated from the numerical model indicates that the best fit simulations are those where the BVG hydraulic conductivity is set to 1.2 m year<sup>-1</sup>, and that the variations in low permeability horizons, faults in the BVG and (within reasonable limits) the cover faults, have very little effect on the good fit produced. This calibration provides the basis for transient mass transport simulations.

## 9. Transient mass transport modelling

The use of OILGEN to simulate transient mass transport has been outlined earlier. This feature of the code was used to provide a visual guide to the degree of physical containment that the BVG and overlying sediments may afford. Any effects of enhanced flow due to thermal buoyancy of water from a warm repository, or vertical leakoff of H<sub>2</sub>, CH<sub>4</sub> and CO<sub>2</sub> gases generated from the repository are ignored (Chapman, 1994). The particles have zero mass and once the steady state flow field is established, a number of particles are released from a specific point and tracked through time across the model. Since they have the same buoyancy as the ambient fluid, they are passive indicators of the groundwater flow path and indicate the actual time that repository fluids would take to reach the surface. The simulations were run with the BVG set to the best match 1.2 m year<sup>-1</sup> hydraulic conductivity (outlined above).

Fluid flow through porous media, or through fractures, usually moves preferentially along the highest conductivity conduits, rather than uniformly through the whole anisotropic medium. Consequently, this “average” modelling will tend to underestimate maximum flow rates. The code is run iteratively to achieve the tracking simulations, with a time step of just 3 years for each iteration. This ensures that a tracer particle does not jump between finite element cells. Five hundred tracking particles were “released” at one time.

Values of storage coefficient, and longitudinal and transverse dispersivity are given in Table 1. As can be seen in Fig. 13, the best-fit head calibration model produced a simulation where water from the repository zone could reach the surface within 15 000 years. Breakthrough of water from the BVG to overlying sediments occurs predominantly via the major fault zone to the west of the repository [equivalent to fault F1 in earlier published reports (Nirex, 1992a)]. A lower conductivity for the BVG resulted in much longer containment of water. Repository water would take 200 000 year to reach the surface, having moved laterally through the St Bees sandstone and into the Calder sandstone before discharging onto the present-day sea bed. There is a possibility that flow might not reach the sea-bed at all if the section were extended and the no-flow boundary at the western edge was relaxed. Thus, the regional BVG hydraulic conductivity is crucial. It is difficult to measure or estimate regional BVG hydraulic conductivity in connected fractures with sufficient certainty (Nirex, 1993a).

## 10. Safety case implications

A simple calculation to illustrate a safety case can be made from the graphic expression of the relationship between water flow to BVG hydraulic conductivity (Fig. 14). It is emphasised that this does not replace the complex interaction of many parameters used by UK Nirex Ltd in their calculations of safety. By contrast, this simplistically illustrates the impact of hydrogeology on overall safety. Assuming that it is unacceptable for water from the repository, at 650 m bOD, to return to the surface within 10 000 year, the flow rate would need to be less than  $6.50 \times 10^{-2}$  m year<sup>-1</sup> to be acceptable. Using Fig. 14, this flow rate equates to a regional BVG hydraulic conductivity of  $3.16 \times 10^{-2}$  m year<sup>-1</sup>. If measured BVG hydraulic conductivities exceed this value, the hydrogeological safety of a 650 m repository could be doubted. Superimposed on Fig. 14 are the range of BVG hydraulic conductivities measured in boreholes at 400–1900 m bOD (Nirex, 1993a,b). It is apparent that measured values are around 1000 times too large to be simply declared “safe”.

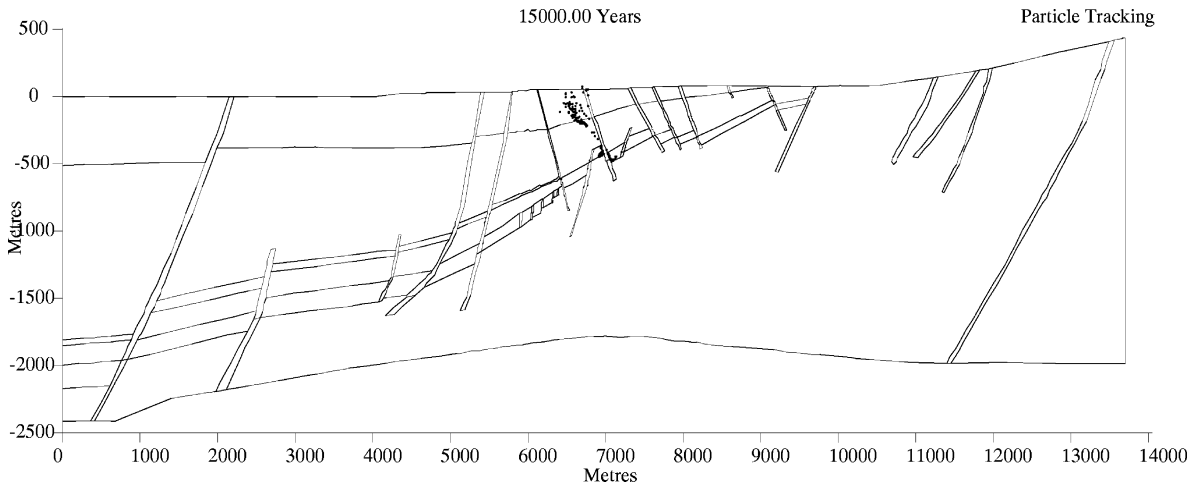


Fig. 13. Result of transient mass transport simulation to track 500 particles released from potential repository. All parameters as those of “base-case” (Table 1), except BVG hydraulic conductivity [set to “best match” of 1.2 m year<sup>-1</sup> hydraulic conductivity (Fig. 11)].

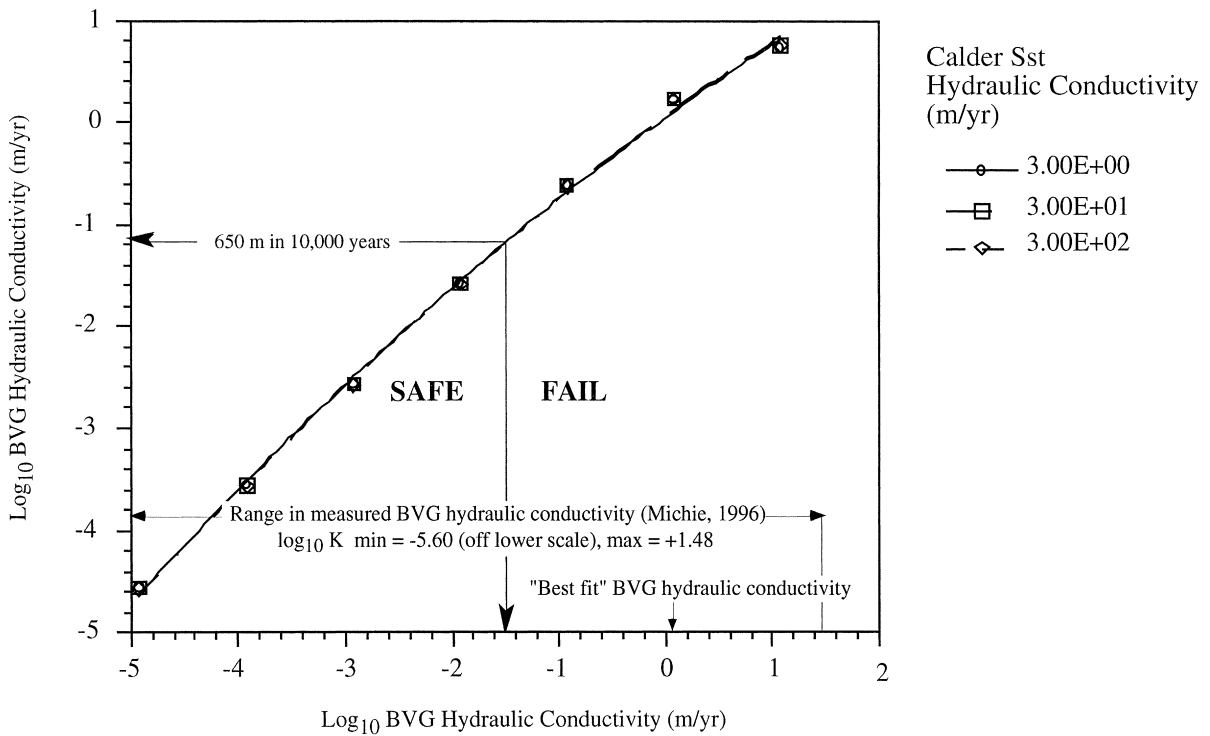


Fig. 14. Simplistic safety case derived from Fig. 9. BVG hydraulic conductivity producing “best match” head comparison (Fig. 11) falls within fail region ( $K=1.2$  m year<sup>-1</sup>,  $\log_{10}K=0.08$ ).

## 11. Conclusions

- The fluid flow simulation code provides a robust indication of the movement directions of groundwater. Even the simplistic simulations show water flow to be topographically driven and upward trending in the central (repository) area of the region.
- The anisotropy of the Borrowdale volcanic group (BVG) and hydraulic conductivity of the St Bees sandstone, St Bees evaporites, Brockram breccia cover faults and faults in the BVG are unimportant relating to repository flow rates; the inclusion of faults and variable salinity are important.
- Geologically complex simulations produce similar results to those of the more simplistic modelling. This indicates that the shape and size of the finite element cells is not relevant to either the flow rate or the flow path, nor, indeed to the numerical solution of the flow and heat transport equations, lending confidence in the OILGEN code.
- Two decoupled, but connected, aquifer systems exist: in the Calder sandstone and in the BVG. Comparison of measured and calculated freshwater hydraulic heads indicates that the best fit simulation is one where the BVG hydraulic conductivity is  $1.2 \text{ m year}^{-1}$ .
- This best fit is not affected by variations in hydraulic conductivity of low permeability units, faults in the BVG or, within reason, faults in the cover sequence. When the permeabilities of the overlying sediments are set to their median, or “base case” values, there is a good fit between measured and calculated freshwater hydraulic heads.
- Newer measured data of BVG hydraulic conductivity shows that some flow rates of the BVG can be 1000 times too permeable to be acceptable. Flow rates through the proposed repository site are predicted to be around  $1.7 \text{ m year}^{-1}$ .
- The proposed repository at 650 m bOD would have been in a poor position where flow directions in the BVG are towards the surface, an effect that would need to be counteracted.
- Simulated tracking of water particles released from the repository zone shows that radionuclides could return to the surface within 15 000 years, if regional hydraulic conductivity of the BVG is equivalent to  $1.2 \text{ m year}^{-1}$ . This assumes that no chemical retardation occurs within the engineered repository, or within the overlying rock.

## Acknowledgments

Chris McKeown was funded by the Greenpeace Environmental Trust. The OILGEN code was kindly provided by Grant Garven. UK Nirex Ltd are thanked for providing data.

## References

- Andrews-Speed, C.P., Oxburgh, E.R., Cooper, B.A., 1984. Temperature and depth-dependent heat-flow in the Western North Sea. *Bulletin of the American Association of Petroleum Geologists* 68 (11), 1764–1781.
- Bachu, S., 1994. Flow of variable-density formation water in deep sloping aquifers: reviews of methods of representation with case studies. *Journal of Hydrology* 164, 19–38.
- Bear, J., 1972. *Dynamics of Fluids in Porous Media*, Environmental Science Series. Elsevier, New York, 764 pp.
- Black, J.H., 1995. The Hydrogeology of the Sellafield Area; the Geological Disposal of Radioactive Waste. IBC Technical Services Ltd, Gilmoora House, 57–61 Mortimer St., London, Royal Lancaster Hotel, London.
- Black, J.H., Brightman, M.A., 1996. Conceptual model of hydrogeology of Sellafield. *Quarterly Journal of Engineering Geology* 29 (Suppl. 1), S83–S93.
- Brace, W.F., 1980. Permeability of crystalline and argillaceous rocks. *International Journal of Rock Mechanics, Mineral Science and Geomechanics Abstracts* 17, 241–251.
- Chadwick, R.A., Kirby, G.A., Baily, H.E., 1994. The post-Triassic structural evolution of north-west England and adjacent parts of the East Irish Sea. *Proceedings of the Yorkshire Geological Society* 50, 99–102.
- Chaplow, R., 1995. Proof of Evidence. *Geology and Hydrogeology*. RCF Planning Enquiry, PE/NRX/14. UK Nirex Ltd., Harwell, UK, Cleator Moor, Cumbria, 72 pp.
- Chapman, N.A., 1994. The geologist’s dilemma: predicting the future behaviour of buried radioactive wastes. *Terra Nova* 6, 5–19.
- Chapman, N.A., McEwen, T.J., 1986. Geological environments for deep disposal of intermediate level wastes in the United Kingdom. In: IAEA (Ed.), *Siting, Design and Construction of Underground Repositories for Radioactive Wastes*.

- International Atomic Energy Authority, Vienna, Austria, pp. 311–328.
- Clauser, C., 1992. Permeability of crystalline rocks. *Transactions American Geophysical Union* 73 (21), 233–238.
- Couples, G.D., McKeown, C., Haszeldine, R.S., Smythe, D.K., 1998. The role of academic environmental geoscientists in radioactive waste disposal assessment. In: Bennett, M.R., Doyle, P. (Eds.), *Issues in Environmental Geology: a British Perspective*. The Geological Society, London, pp. 243–276.
- de Marsily, G., 1986. *Quantitative Hydrogeology. Groundwater Hydrology for Engineers*. Academic Press, London, 440 pp.
- Deming, D., Sass, J.H., Lachenbruch, A.H., De Rito, R.F., 1992. Heat flow and subsurface temperature as evidence for basin-scale groundwater flow, North Slope Alaska. *Bulletin of the Geological Society of America* 104, 528–542.
- Follin, S., Thunkin, R., 1994. On the use of continuum approximations for regional modeling of groundwater flow in crystalline rocks. *Advances in Water Resources* 17, 133–134.
- Garven, G., 1989. A hydrogeologic model for the formation of the giant oil sands deposits of the Western Canadian sedimentary basin. *American Journal of Science* 289, 105–166.
- Garven, G., 1994. Genesis of stratabound ore deposits in the midcontinent basins of North America. 1. The role of regional groundwater flow — a reply. *American Journal of Science* 294, 760–765.
- Haszeldine, R.S., McKeown, C., 1995. A model approach to radioactive waste disposal at Sellafield. *Terra Nova* 7 (1), 87–96.
- Haszeldine, R.S., Smythe, D.K., 1997. Why was Sellafield rejected as a disposal site for radioactive waste? *Geoscientist* 7, 18–20.
- Heathcote, J.A., Jones, M.A., Herbert, A.W., 1996. Modelling groundwater flow in the Sellafield area. *Quarterly Journal of Engineering Geology* 29 (Suppl. 1), S59–S81.
- Huyakorn, P.S., Pinder, G.F., 1983. *Computational Methods in Subsurface Flow*. Academic Press, London, 473 pp.
- Kazda, I., 1990. *Finite Element Techniques in Groundwater Flow Studies with Applications in Hydraulic and Geotechnical Engineering*. Elsevier, Amsterdam, 313 pp.
- Kestin, J., Khalifa, H.E., Correia, R.J., 1981. Tables of the dynamic and kinematic viscosity of aqueous NaCl solutions in the temperature range 20–150°C and the pressure range of 0.1–35 MPa. *Journal Physical Chemical Reference Data* 10, 71–87.
- LaBolle, E.M., Fogg, G.E., Tompson, A.F.B., 1996. Random-walk simulation of transport in heterogeneous porous media: local mass-conservation problem and conservation methods. *Water Resources Research* 32 (3), 583–593.
- Lerche, I., 1990. *Basin Analysis — Quantitative Methods*, vol. 1. Academic Press, San Diego, 562 pp.
- Littleboy, A., 1996. The geology and hydrogeology of the Sellafield area: development of the way forward. *Quarterly Journal of Engineering Geology* 29 (Suppl. 1), S95–S104.
- Luszczynski, N.J., 1961. Head and flow of ground water of variable density. *Journal of Geophysical Research* 66 (12), 4247–4256.
- McDonald, C.S., Jarvis, C., Knipe, C.V., 1996. RCF planning appeal by UK Nirex Ltd. Report No. APP/HO900/A/94/247019, DOE.
- McKeown, C., 1997. A model approach to radioactive waste disposal at Sellafield. PhD Thesis, University of Glasgow, Glasgow, 262 pp.
- McKeown, C., Haszeldine, R.S., 1995. *Modelling Groundwater Flow and Chemistry in the Proposed Repository Zone; the Geological Disposal of Radioactive Waste*. IBC Technical Services Ltd, Gilmoora House, 57–61 Mortimer St., London, Royal Lancaster Hotel, London.
- Michie, U., 1996. The geological framework of the Sellafield area and its relationship to hydrogeology. *Quarterly Journal of Engineering Geology* 29 (Suppl. 1), S13–S27.
- Michie, U.M., Bowden, R.A., 1994. UK Nirex geological investigations at Sellafield. *Proceedings of the Yorkshire Geological Society* 50, 5–9.
- Moreno, L., Neretnieks, I., 1993. Fluid flow and solute transport in a network of channels. *Journal of Contaminant Hydrology* 14, 163–192.
- Neumann, S.P., 1990. Universal scaling of hydraulic conductivities and dispersivities in geologic media. *Water Resources Research* 26, 1749–1758.
- Nicholls, D.B., 1995. *Hydrogeological Modelling of the Sellafield Site*, vols. I and II (text and appendices). Report No. TR-Z2-7, Her Majesty's Inspectorate of Pollution, London, UK.
- Nirex, 1992a. *The Geology and Hydrogeology of Sellafield*. Report no. 263, UK Nirex Ltd., Harwell, UK.
- Nirex, 1992b. *Sellafield Hydrogeology*. Report of the hydrogeology joint interpretation team. Report no. 268, UK Nirex Ltd., Harwell, UK.
- Nirex, 1993a. *The Geology and Hydrogeology of the Sellafield Area: Interim Assessment*. Report no. 524 (4 vols.), UK Nirex Ltd., Harwell, UK.
- Nirex, 1993b. *Scientific Update 1993: Nirex Deep Waste Repository Project*. Report no. 525, UK Nirex Ltd., Harwell, UK.
- Nirex, 1995a. *Post-closure Performance Assessment, Near-field Evolution*. Report no. S/95/009, UK Nirex Ltd., Harwell, UK.
- Nirex, 1995b. *A Preliminary Analysis of the Groundwater Pathway for a Deep Repository at Sellafield*. Report no. S/95/012 (3 vols.), UK Nirex Ltd., Harwell, UK.
- Nirex, 1997. *The Hydrogeology of the Sellafield Area: 1997 Update*. Report no. S/97/008, UK Nirex Ltd., Harwell, UK.
- Petterson, M.G., Beddoe-Stephens, B., Millward, D., Johnson, E.W., 1992. A pre-caldera plateau-andesite field in the Borrowdale volcanic group of the English Lake District. *Journal of the Geological Society of London* 149, 889–906.
- Raffensperger, J.P., Garven, G., 1995. The formation of unconformity-type uranium deposits. 1. Coupled groundwater flow and transport modeling. *American Journal of Science* 295, 581–636.
- Smythe, D.K., 1996. The 3-D structural geology of the PRZ. Proof of evidence. In: Haszeldine, R.S., Smythe, D.K. (Eds.), *Radioactive Waste Disposal at Sellafield, UK. Site Selection, Geological and Engineering Problems*. University of Glasgow, Glasgow, UK, pp. 237–278.
- Taylor, B.J., Burgess, I.C., Land, D.H., Mills, D.A.C., Smith, D.B., Warren, M.A., 1971. *Geology of Northern England*. HMSO, London, 121 pp.